

Peter J. Sousounis*, H. He, M. L. Healy, V. K. Jain, G. Ljung, Y. Qu, and B. Shen-Tu
AIR Worldwide Corporation, Boston, MA

1. INTRODUCTION

Nowhere else in the world do tropical cyclones (TCs) develop more frequently than in the Northwest Pacific Basin. Nearly thirty TCs are spawned each year, 20 of which reach hurricane or typhoon status (cf. Fig. 1). Five of these reach super typhoon status, with windspeeds over 130 kts. In contrast, the North Atlantic typically generates only ten TCs, seven of which reach hurricane status.

Additionally, there is no other country in the world where TCs strike with more frequency than in China. Nearly ten landfalling TCs occur in a typical year, with one to two additional by-passing storms coming close enough to the coast to cause damage. The high landfall frequency is a result of China being at the western edge of the Northwest Pacific Basin and to the fact that China has a coastline extending nearly 14,000 km in a north-south direction and spanning nearly 30 degrees of latitude - from 18 N to 45 N.

These tropical cyclones, or typhoons as they are called in that part of the world, cause considerable damage. Over just a recent 16 year period, from 1989 to 2005, economic losses totaling in the billions of US dollars have occurred in the coastal provinces of Jiangsu, Zhejiang, and Fujian (Guy Carpenter, 2006). Zhejiang has actually been the province with the highest losses since 1989 (cf. Fig. 2). The heavy loss is a combined result of high exposure and impact from strong typhoons.

The word typhoon stems from the Chinese *jufeng* which originated in 5th century Chinese literature to mean "a wind coming from four directions" (cf. p. 19-20 in Emanuel 2005). Typhoons in China certainly cause significant damage because of their wind. But typhoons are also responsible for considerable damage from flooding that results from torrential rainfall. The significance of flood damage from typhoons is most recently highlighted by comparing two typhoons that impacted China in 2006: Bilis and Saomai. Saomai affected Zhejiang and Fujian Provinces and is perhaps the more showcased of

the two. Because of its wind intensity (135 mph maximum sustained winds), it has been compared to Hurricane Katrina 2005. But Saomai was short lived, and although it made landfall as a strong Category 4 storm and generated heavy precipitation, it weakened quickly. Still, economic losses were ~12 B RMB (~1.5 B USD). In contrast, Bilis, which made landfall a month earlier just south of where Saomai hit, was actually only tropical storm strength at landfall with max sustained winds of 70 mph. Bilis weakened further still upon landfall but turned southwest and traveled slowly over a period of five days across Hunan, Guangdong, Guangxi and Yunnan Provinces. It generated copious amounts of precipitation, with large areas receiving more than 300 mm. Bilis was responsible for ~28 B RMB (~3.5 B USD) of economic loss. Bilis had half the winds of Saomai but generated twice the loss. Bilis affected six provinces and Saomai affected three.

While China has had a long history of significant typhoon losses, the insurance industry targeted toward these disasters is still in its infancy. Worldwide, the Chinese non-life insurance market was only the 12th largest in 2005. However, within Asia, China ranked 3rd in Life and Non-Life Insurance Premiums for the same time (Int'l Ins. Fact Book 2006). Figure 3 indicates Non-Life Insurance Premiums were 10.7 B USD in 2003. Despite its high ranking in Asia, China accounted for only 1.4% of global non-life insurance premium income in 2005.

Insurance Premium Growth in China however is among the highest in Asia. Non Life Per Capita Premiums in China have doubled from 2001 to 2005. Only Thailand and Indonesia have enjoyed higher growth rates (Benfield Group Ltd, 2006).

AIR-Worldwide Corporation is a catastrophe modeling firm located in Boston, MA. Its mission is to develop models and provide information for use by the insurance industry for understanding risk from Natural and Man-Made Hazards.

Founded in 1987, AIR pioneered the probabilistic catastrophe modeling technology that revolutionized the way insurers, reinsurers and financial institutions manage their catastrophe risk. The models developed at AIR enable companies to identify, quantify, and plan

* Corresponding author address: Peter J. Sousounis, AIR-Worldwide Corporation., 131 Dartmouth Street, Boston, MA 02116; email: psousounis@air-worldwide.com.

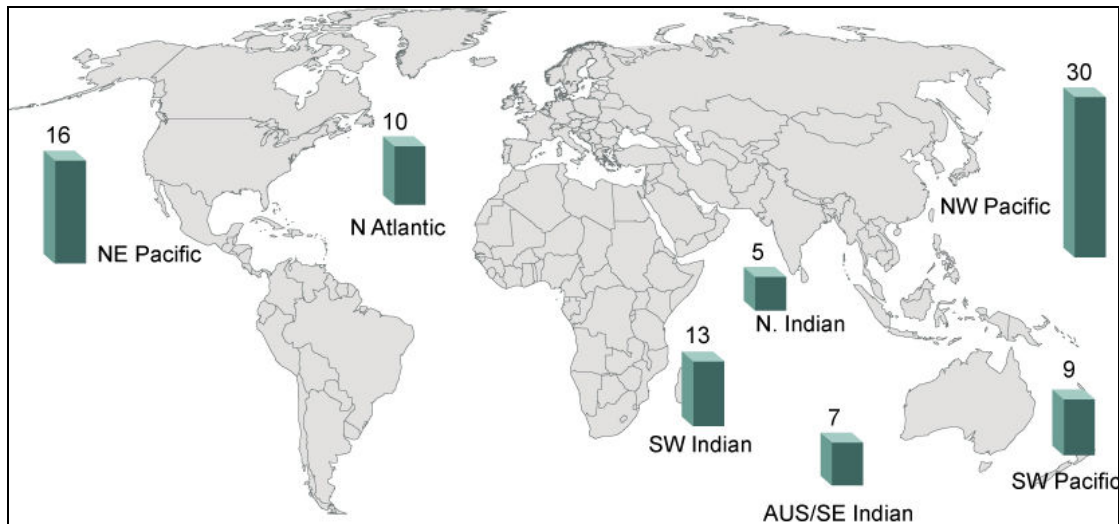


Fig 1. Tropical Cyclone Formation (Wind Speeds > 63 km/h) by Ocean Basin.

for the financial consequences of catastrophic events.

AIR has developed risk models for hurricanes, earthquakes, winter storms, tornadoes, hailstorms, wildfires, and flood, for more than 40 countries throughout North America, the Caribbean, South America, Europe and the Asia-Pacific region. Recently, AIR developed a China Typhoon Model to understand tropical cyclone risk in that country.

The following sections provide an overview of the China Typhoon Model components, the regionally specific meteorological and hydrological aspects of the model, and results that highlight the typhoon risk in China.

2. GENERAL STRUCTURE OF CATASTROPHE MODELS

Most catastrophe models (or cat Models for short) share three common elements. The hazard component first models the frequency, intensity and duration, if applicable, of the peril that is responsible for the damage. The engineering or damage component then determines the fraction of the building(s) in affected areas including their contents that have been damaged. Finally, a loss estimation component computes insured losses by applying the policy conditions to the total damage estimates. Policy conditions may include deductibles by coverage, site-specific or blanket deductibles, coverage limits and sub-limits, loss triggers, coinsurance, attachment points and limits for single or multiple location policies, and risk specific reinsurance terms.

For estimation of insured losses, two important input data files are the event catalog and the exposure file. The catalog file provides a complete list of synthesized (e.g., stochastic) events along with their attributes over a 10,000 year period representing 10,000 scenarios of storm activity that could occur in any given year. The second file, the exposure file, contains area averaged information about building types, construction materials, construction designs, occupancy, and height, as well as total replacement values for the buildings and associated contents. In addition to an industry exposure file that is developed internally, exposure files are often supplied by an insurance or re-insurance client who is interested in knowing what the potential losses would be on their particular portfolio.

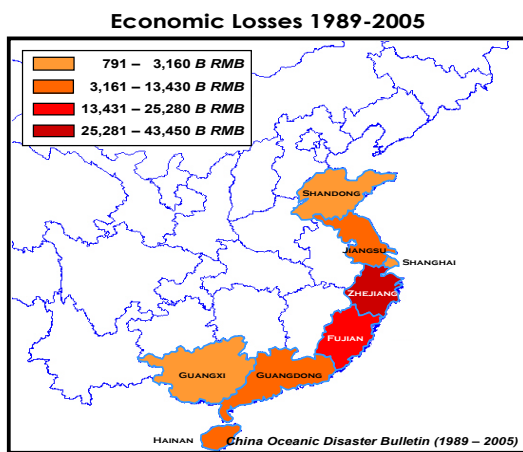


Fig. 2. Economic Losses in China from Typhoons as reported in China Oceanic Disaster Bulletin.

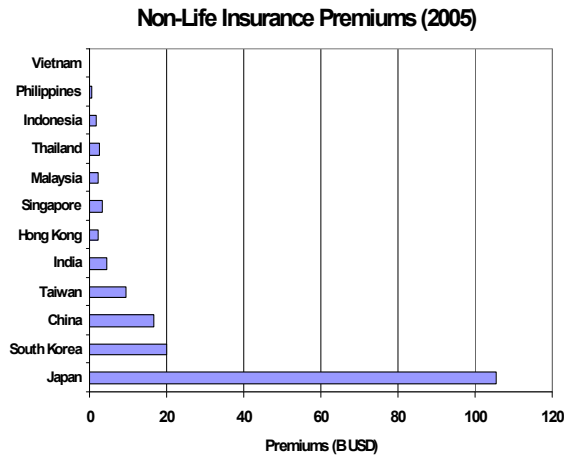


Fig. 3. Non-life insurance premiums in billions of US dollars for 2005 for selected countries in Asia.

For tropical cyclone models, the stochastic storm tracks are generated using probability models that are developed and based on historical information. Specifically, stochastic storms are generated by first drawing a starting point probabilistically over the Northwest Pacific Ocean, for example. The initial track direction of the storm, as well as forward speed, intensity and radius of maximum winds are assigned according to the probability distribution derived from historical data. Time series models are then used to simulate storm path and characteristics along the path – basically to move the storm forward. This process is repeated for every 6-hourly point. This way a potential typhoon is generated with hourly information. The algorithm automatically determines whether the storm makes landfall. With this Monte Carlo method, potential typhoons are generated for hundreds and thousands of years. The collection of possible events is called a stochastic catalog.

To determine statistically sound loss estimates, the stochastic events are then processed within the hazard component to obtain local intensity estimates for each event. In the AIR tropical cyclone models, the hourly track information is used to compute one-minute sustained windspeeds at all points of interest from an exposure perspective. The windspeed at a given location is computed by determining the gradient windspeed at that point based on the distance from the storm center, latitude, storm size, and central pressure. The gradient wind is then converted to a surface wind by first reducing the 10-minute gradient wind value (e.g., at 850 mb) over water to a 10-meter 10-minute wind over water. The storm motion is included to yield an asymmetric wind pattern with higher speeds on the right and lower speeds on the left. That wind is further modified to account for the effects

of friction, terrain, and shorter-period gusts using high resolution land use/land cover and digital-elevation data to obtain a 1-minute 10-meter wind over land.

Windspeeds are computed at every hour of the storm's lifetime for all exposure points and stored as necessary. Very weak winds are ignored as they do not contribute to damage. Thus, for each location in question, a temporal profile of damaging winds is produced for use in the other two model components.

In the damage component of the model, the temporal profile is used in conjunction with the relevant exposure information and proprietary damage functions (DFs) developed at AIR. These DFs account for the fact that different types of buildings behave differently under strong wind conditions. Building types are based on construction material as well as occupancy class and height. For example, a three-story wooden residential structure will be much more susceptible to wind damage than a one-story commercial steel structure.

At each exposure point, the fractional damage of the building and its contents as well as additional time-element related damage is computed. Time-element damage is that which relates to a business possibly being disrupted for some time following the event. If a flood component is included in the tropical cyclone model, as is the case here with the AIR China Typhoon Model, then that damage is determined in a similar way, with flood depth information rather than windspeed information, and with flood DFs rather than wind DFs. The flood component will be discussed in more detail in the next section.

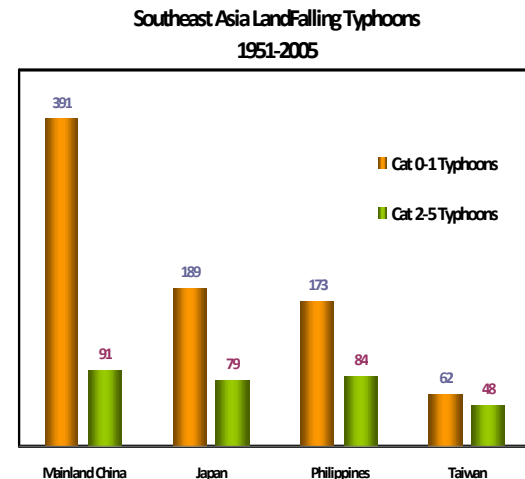


Fig. 4. Regional landfall frequencies of weak and strong typhoons for selected countries in Southeast Asia.

3. CHINA-SPECIFIC CONSIDERATIONS

While the basic components of tropical cyclone catastrophe models developed at AIR may be similar across the various regions for which they were developed, regionally specific geographical features or meteorological conditions usually require more than simple modifications of input files to adequately incorporate the regional uniqueness.

3.1 importance of weak events

For example, because of a focus on flooding with the China Typhoon Model, and because there is generally little correlation between storm central pressure and rainfall potential, it was necessary to include weak typhoons in the model formulation. Thus all storms of tropical storm strength or greater, from 1951 to 2005, were included in the development of the stochastic catalog. Figure 4 shows the distribution of weak typhoons making landfall in China with respect to other Southeast Asia countries.

The need to include weak storms presented a problem on two fronts. First, an Agency like the Japanese Meteorological Agency (JMA) or the Joint Typhoon Warning Center (JTWC) does not necessarily track all such weak (tropical) storms, so an additional source of track information was necessary. Second, many agencies, even for strong storms at landfall, stop tracking them when they weaken below tropical storm strength – even if they remain hydrologically significant.

Track data from the Shanghai Typhoon Institute (STI) was therefore obtained via a collaborative effort to better understand the impacts of typhoons in China. The STI data contained a more comprehensive set of storms that impacted China than either JTWC or even JMA. Additionally, the tracks tended to be longer. It was invaluable for developing the stochastic catalog. An example of the utility that the STI data provided over that from other agencies is shown in Fig. 5 for one event - Fitow 2000.

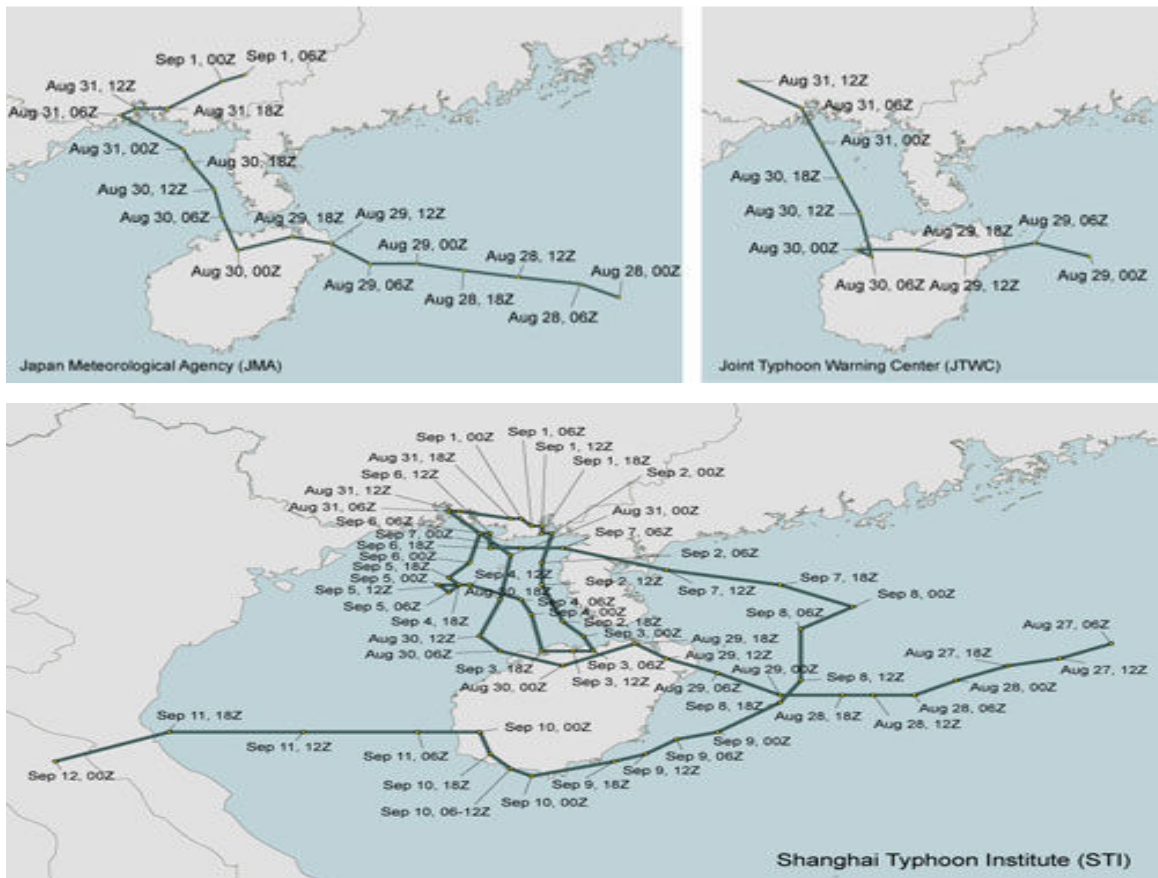


Fig. 5. Comparison of track information from three different typhoon agencies for Fitow 2000 as shown.

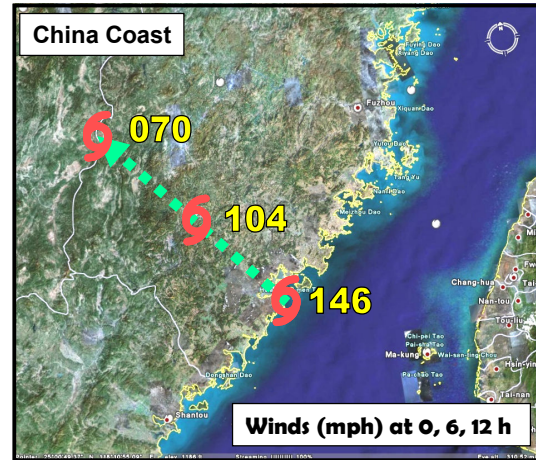
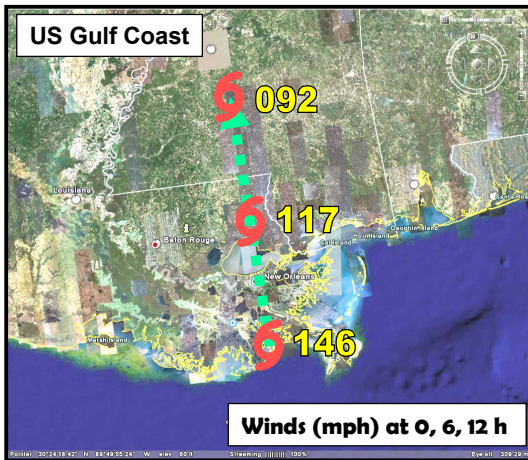


Fig. 6. Comparison of inland dissipation of winds for strong hurricanes (920-945 mb) as they make landfall along the U.S. Gulf Coast (left) and Southeast China coast (right).

3.2 inland filling

China's terrain is characterized by several significant mountain ranges in the southeast part. These mountains begin within several tens of kilometers from the coast and extend inland for many hundreds of kilometers. Typical peak elevations are around 2000 m. These coastal mountains have a significant role on both the wind and precipitation aspects of typhoons.

For example, Fig. 6 shows an average picture of how winds dissipate in strong hurricanes (920-945 mb) as they make landfall along the Gulf Coast of the US and along the southeast coast of China. Along the Gulf Coast, over a period of twelve hours, winds drop from 146 mph to 92 mph. In China, because of the significant mountain ranges located near the coast, typhoons weaken more quickly. Over a twelve hour period, the average picture for the same intensity storm shows that winds drop from 146 to 70 mph. As a specific example, Typhoon Saomai made landfall with winds near 135 mph but by 12 hours later winds had diminished to 56 mph.

This weakening, or filling effect was incorporated into the AIR China Typhoon Model by examining the post-landfall evolution of central pressures in typhoons using the STI track data. A latitude- and intensity-based relationship was obtained that was then applied to all the stochastic events in the 10,000 year catalog. Note that when the model is used in real time and/or on real storms, the actual (post-landfall) storm intensity is used.

3.3 precipitation influences

The conceptual model of a circularly symmetric typhoon and its associated and

correspondingly simple precipitation shield breaks down as storms approach China. The breakdown occurs primarily because of the complicated terrain and an influence of the South China Sea Monsoon, but also because storms can form at almost any time of the year and interact with approaching mid-latitude weather systems. Thus, the precipitation shield takes on a much more complicated and very asymmetric shape. A typical result is shown in Fig. 7 with Typhoon Nathan 1990. Long before Nathan actually reached mainland China, clouds and heavy precipitation developed ahead of and well north of the center (not shown). Nathan made landfall just north of Hainan Province but clouds and precipitation extend well north – even beyond Taiwan. As a result, the precipitation maximum of 387 mm occurred nearly 700 km away - to the north.

The precipitation enhancement on the north side of typhoons approaching China occurs because the counterclockwise flow around the storm is onshore. This flow decelerates as it moves over the relatively rougher surface and ascends the coastal mountains. The rising air (otherwise known as orographic lifting), cools and the moisture condenses to form clouds and precipitation. The magnitude of the orographic enhancement is proportional to the speed of the wind and the upslope angle of the terrain.

An almost opposite effect occurs on the south side of typhoons. On this side, the counterclockwise flow is offshore. As air moves down the mountains, it warms and dries - actually eroding the cloudiness. The northward enhancement and southward erosion accentuate the asymmetric evolution of the precipitation footprint.

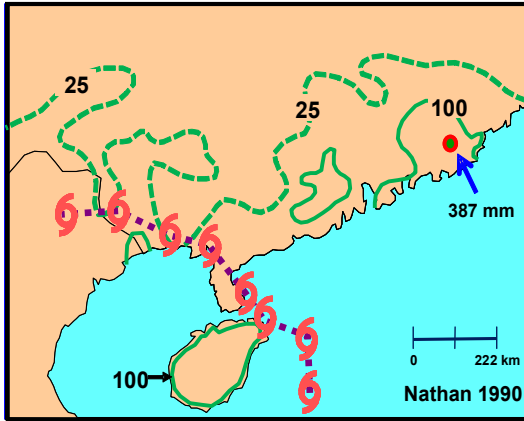


Fig. 7. Track of Typhoon Nathan and selected precipitation contours and location of precipitation maximum shown.

The South China Sea Monsoon (SCSM) can also have an effect on precipitation after a typhoon makes landfall. The SCSM is an annual occurrence and is responsible for pumping lots of tropical moisture northward across southeastern provinces in China (Chang and Chen 1995). Each year in spring, the Asian continent begins to warm more rapidly than the surrounding South China Sea. As that warm air rises, it is replaced

by a slightly cooler but much moister flow from the southwest. In late fall, the opposite flow develops from the northeast as the land begins its wintertime cooling. The strength of the summertime southwesterly flow, like many other climate signals, varies from year to year. Depending on the strength of the monsoonal pumping at any given time, and nearby weather systems – copious amounts of precipitation can be triggered.

Recall Bilis, which made landfall as a tropical storm but wreaked havoc in terms of precipitation for the next five days. Many areas received over 300 mm of precipitation. Figure 8 shows how the clouds and corresponding precipitation shield shifted dramatically and abruptly to the south as Bilis made landfall. Bilis made landfall north of Taiwan and headed inland initially in a WNW direction. But, shortly after landfall, Bilis changed direction abruptly to the southwest. The enhanced cloudiness and increased precipitation that developed to the southwest in the next few days following Bilis' landfall demonstrates the interaction of the tropical storm with the SCSM (Yihong, 2006).

Other regional weather systems can also influence the evolution of typhoons once they make landfall. In early August of 1975, Super

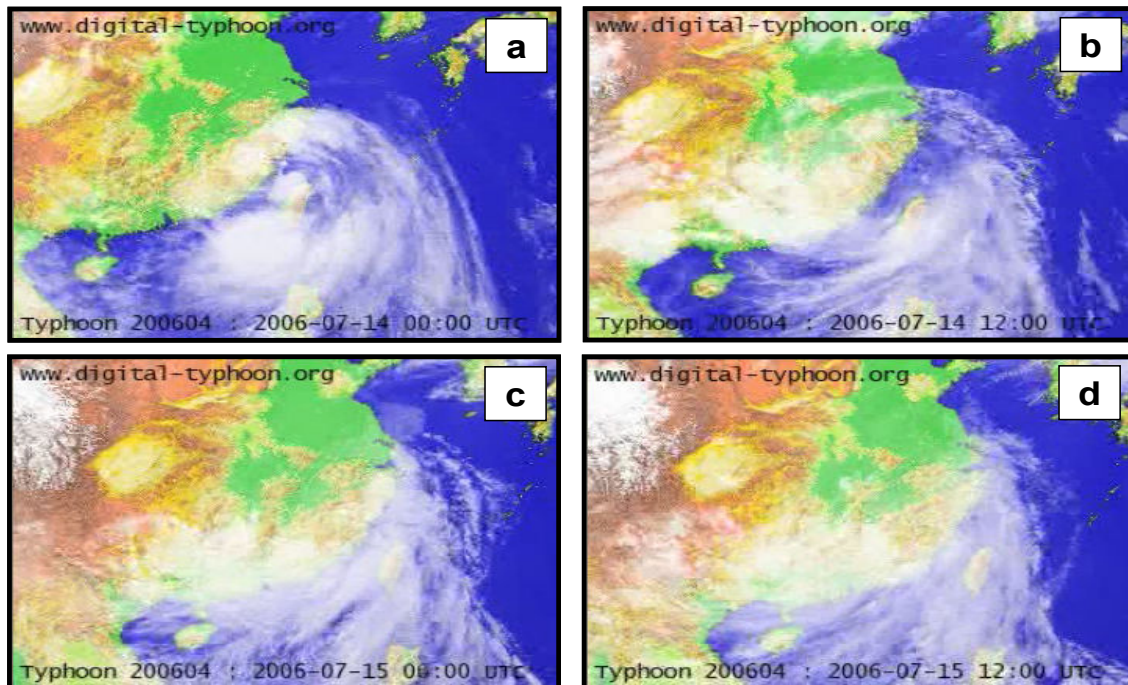


Fig. 8. Satellite images of Bilis crossing China coastline at times shown. See text for details.

Typhoon Nina made landfall along the coast of Fujian late. Maximum sustained windspeeds at landfall were 90 mph and decayed rapidly to less than 40 mph within 12 hours. However, Nina kept moving inland for nearly 84 more hours, generating record breaking amounts of precipitation and subsequently became one of the most catastrophic storms in terms of loss of life in modern China History. One station reported 1062 mm in 24 hours. The Banqiao and Shemantan Dams, which were designed for 1000 year events on the Ru River both broke and unleashed water at an unprecedented rate. Nearly 200,000 fatalities occurred as a result of the floodwaters. (Quing et al. 1997)

Sometimes an approaching weather system and/or the steering flow can influence a typhoon to recurve shortly after landfall towards the northeast and transform more significantly from a tropical to an extratropical system. The result is a dramatic and rapid evolution from a circularly symmetric cloud mass to a comma-shaped cloud mass. Heavy precipitation then shifts from a more or less concentric ring near the center to being distributed in two elongated bands corresponding to the cold and warm fronts of the developing extratropical system.

Extratropical transition occurs most frequently in August and September because cold air masses are able to penetrate farther south going into the Fall season and typhoons are still powerful enough to take advantage of the additional energy source provided from the horizontal temperature contrast (Jones et al.

2003). Extratropical transition is also accounted for in the model wind field. Specifically, the model accounts for an increase in winds on the east or right side of the typhoon by increasing the forward speed, which is a noted characteristic of these systems.

Careful analysis of satellite imagery and event precipitation footprints provided by STI led to the development of a precipitation model for the China Typhoon Model. The precipitation model captures the impacts that Taiwan and the coastal mountains have on the precipitation footprint. It also allows for evolution of precipitation intensity as the storm moves inland. Finally, it allows for the morphological evolution as the storm interacts with the South China Sea Monsoon and other synoptic weather features, as well as extratropical transition.

Figure 9 shows the accumulated precipitation footprint from the AIR China Typhoon Model simulation of Typhoon Fred 1994. This very significant storm was responsible for an estimated 17 B RMB (2.13 B USD) in economic loss (Kentang 2000). Fred was an extratropical transitioning storm, a characteristic that is captured nicely by the model. Note the signature of how the precipitation totals first decreased shortly after landfall but then increased as the storm recurved to the north and east and began to transform into an extratropical one.

3.4 flood considerations

Development and incorporation of the flood model into the AIR China Typhoon Model presented several challenges. The first challenge was one of creating a model that by itself could run reasonably fast. Because the models developed at AIR are run by clients on PCs as opposed to supercomputers, they need to be considerably less complicated than say the MM5 or WRF models. However, at the same time, they must have inherently high resolution to capture the effects of small scale changes in terrain. A spatial resolution of 5 km was found to be a good compromise.

A second challenge was in maintaining the computational speed of the model as a whole. Because floods can occur in regions where precipitation has not even fallen, the incorporation of a flood model required computations to occur everywhere mainland China as well as land mass from adjacent countries existed within a rectangular grid. That constraint thus required computation of precipitation at over one-half million points – even if no exposure existed at certain points.

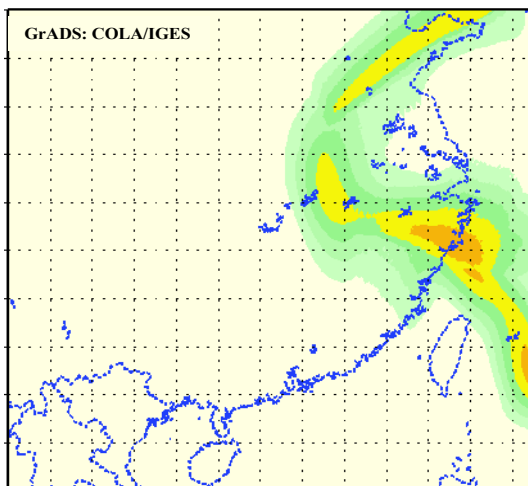


Fig. 9. AIR model-generated precipitation totals for Typhoon Fred 1994. Light precipitation amounts shown in green and heavy precipitation amounts are shown in orange.

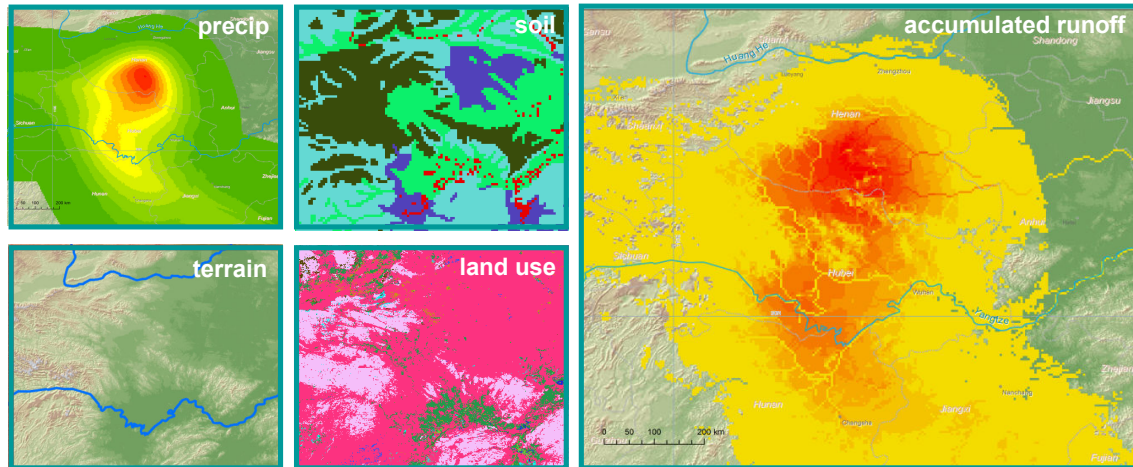


Fig. 10. Sample inputs (small panels) and outputs (large panel) to flood model component of AIR China Typhoon Model.

The flood component works as follows. After the precipitation model component generates total event precipitation, the underlying soil and land use distributions and terrain at 5 km resolutions re-distribute the water. Over the entire model domain and within each 5 km grid cell, a fraction of the precipitation that falls is absorbed depending on the particular soil and land use. If the soil is sandy, a higher fraction will percolate down than if the soil is clay. Similarly, if the land use is forest, then more precipitation will percolate down than if the land use is urban. The remaining amount of the precipitation is then transported downhill to the next cell – in the direction of the steepest gradient. This process occurs across all the cells and each cell experiences an accumulated runoff - typically from many many other cells. The accumulated runoff is then normalized based on the number of contributing cells (e.g., the watershed).

A comparison of the precipitation and accumulated runoff (cf. Fig. 10) illustrates how the flood model will not necessarily cause dramatic redistributions of the precipitation – but it will add realistic high resolution information within the precipitation footprint as to which areas are at higher risk than others.

3.5 exposure and construction types

The most widespread and concentrated exposures in mainland China are located in Jiangsu and Zhejiang Provinces – in and around the cities of Nanjing, Shanghai, and Hangzhou.

In developing an industry exposure database for China, AIR engineers collaborated with the Beijing Institute of Architectural Design to better understand local building designs and

construction materials and practices. Historically, adobe and brick with wood-frame were the predominant construction types for single family homes in China, and they are still widespread in rural areas today. However, these usually poorly engineered structures are generally not insured. Today, confined masonry and reinforced concrete are the predominant construction types for insured single-family homes.

Commercial structures vary from poorly constructed low-rise masonry structures to well-maintained mid- and high-rise reinforced concrete buildings. Concrete and masonry are the primary construction materials. In high rise commercial buildings, steel is only used about one-tenth of the time. Steel is used even less frequently for low- and mid-rise buildings.

A very unique aspect of China's building stock is that a significant portion is represented by buildings under construction. Most of these structures—which constitute the risk category Construction All Risks (CAR) or Erection All Risks (EAR)—are concrete and masonry structures. Since both the replacement value and vulnerability for these structures vary with the construction phase, their vulnerability can be significantly different from that of buildings that are already finished.

3.6 flood vs wind vulnerability

The response of structures to wind and flood loads varies with building material and construction design. The integrity of the building envelope is very important from a wind vulnerability point of view. In masonry construction, connections between different

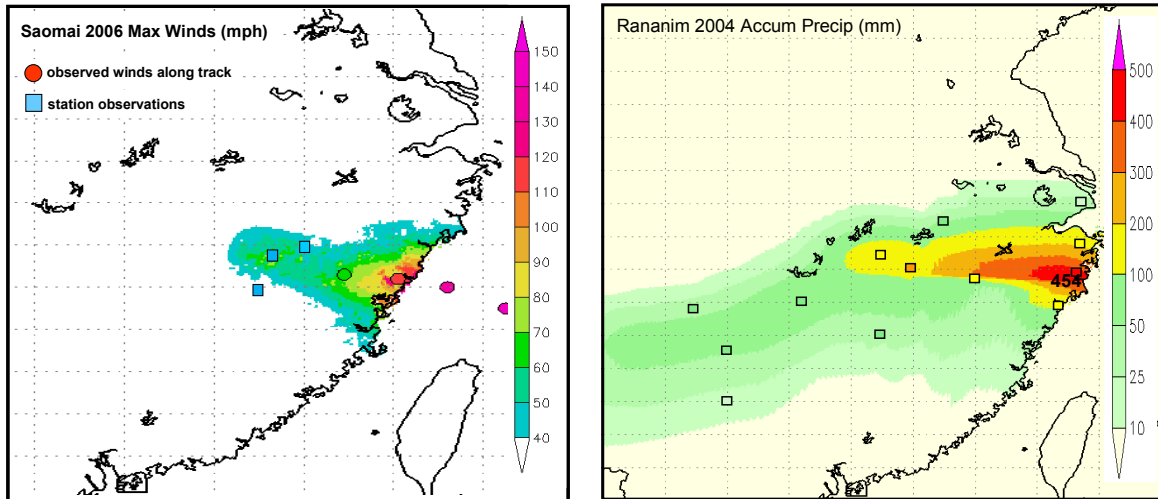


Fig. 11. Comparison of AIR modeled (color filled contours) and observed (symbols) typhoon maximum winds and precipitation totals for events as shown.

building elements such as the roof and the wall are not strong as in steel and concrete frame structures. This makes the masonry construction more susceptible to lateral wind loads. Concrete material is less vulnerable to flood loads than steel and masonry structures.

With the increase in height, wind loads increase. However, high-rise buildings are well designed to counter the increasing loads and generally perform much better than low-rise buildings under wind loads. From a flood hazard perspective, the impact from flood is usually restricted to lower stories of a building. Because high-rise buildings have a higher replacement value than low-rise buildings, this translates into lower damage ratio for high-rise buildings than low-rise buildings.

4. MODEL VALIDATION AND CALIBRATION

The calibration of the AIR China Typhoon Model as with all models developed at AIR was a rigorous and time consuming process. Each component was calibrated separately and the final calibration to the wind and flood DFs was performed based on detailed and proprietary loss information from leading insurance companies in China.

Regarding the hazard component, comparison of observations with modeled winds (or precipitation) is not straightforward. Observations are made at a limited number of sites and their measurements reflect the characteristics of the sensor, including averaging time, sampling rate, etc. Furthermore, the modeled wind speeds are representative of a grid cell area, not a point location. Thus when

validating local intensity calculations, it is really only possible to say to what degree modeled wind speeds are consistent with observations and reproduce the appropriate pattern of maximum winds within a storm system.

Simulated wind and precipitation fields were validated against observations from more than a dozen historical China typhoons. Figure 11 (left panel) shows observed wind speeds for Typhoon Saomai (2006) overlaid on AIR's modeled wind field for this storm. Note the fine scale features in the modeled wind field that result from the local effects discussed earlier. Also note the higher wind speeds on the right-hand side of the storm, resulting from the (easterly) steering flow that is superimposed onto the counterclockwise rotational winds from the typhoon. Figure 11 (right panel) shows observed precipitation totals for Typhoon Rananim (2004) overlaid on AIR's modeled precipitation for this storm. Note the good agreement in maximum event precipitation along the coast as well as in the decreased values farther inland.

5. TYPHOON RISK IN CHINA

Figure 12 (left panel) indicates the distribution of 50 year return period typhoon winds from the AIR China Typhoon Model. The highest-risk area from wind is located due north of Taiwan, near Wenzhou, near where some of the strongest typhoons historically have made landfall. The lowest-risk area from wind along the coast is just to the south - around Fuzhou. This result is also consistent with observations of relatively low frequency of very strong typhoons,

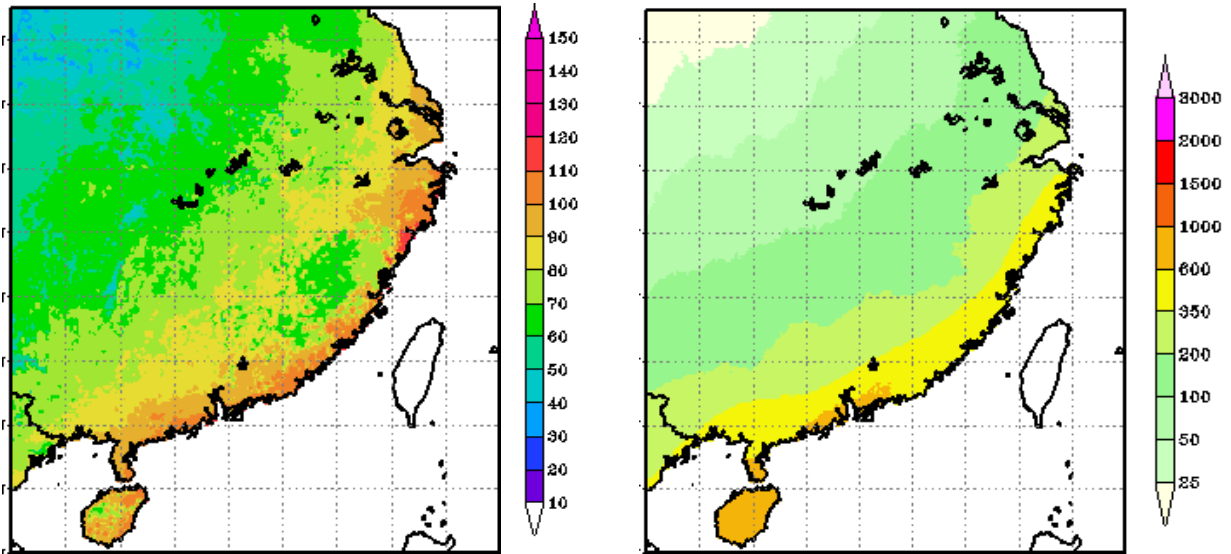


Fig. 12. AIR China Typhoon Model derived 50 year return period winds (mph, left) and precipitation (mm, right).

which is a result of the Taiwan Central Mountain Range.

Figure 12 (right panel) illustrates that the highest (flooding) precipitation risks are in the southeast provinces of Guangdong – along the coast, and Hainan. Return period precipitation for a 2% event, or a 1-in-50 year event is on the order of 450 mm. Farther to the north along the coast, in Shanghai, the threat is considerably diminished. Note that the 100 mm, 50 mm, and 25 mm contours extend inland roughly 600, 900, and 1200 km inland.

The net result of the wind and precipitation (flood) risks together, combined with the distribution of exposure is shown in Fig. 13. The distributed risk reflects the wind-based risk to the north and the flood-based risk to the south.

6. SUMMARY

Precipitation-induced flooding is a major risk from China Typhoons that is covered under standard insurance policies in mainland China. Significant flooding can occur hundreds of kilometers inland and several days after landfall. Weak storms are therefore an important part of China's typhoon climatology. Precipitation evolution is complicated by terrain, the South China Sea Monsoon, weather systems, and extratropical transitioning. AIR recently developed a China Typhoon Model that captures the effects of both wind and flood and accounts for the diverse construction and occupancy types of buildings in China as well as the significant contribution from buildings under construction. The highest risk from wind is a maximum along the coast north of Taiwan because rugged coastal terrain quickly diminishes wind speeds inland. The highest risk from precipitation induced flood is a maximum farther south in Guangdong.

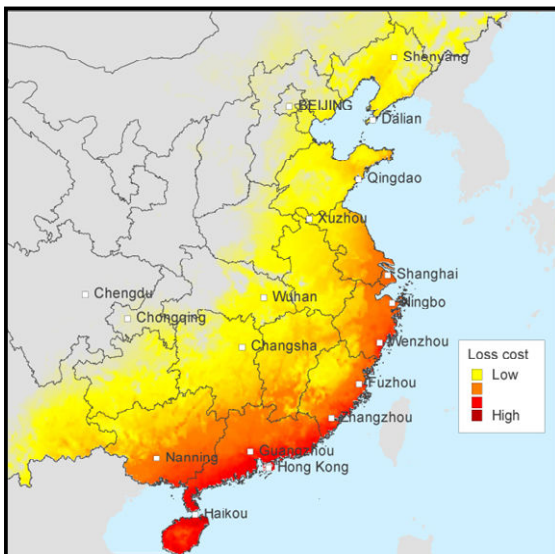


Fig. 13. AIR modeled Typhoon Risk in China.

REFERENCES

Benfield Group Limited, 2006: China Insurance Market Review: Major Changes, Rapid Growth, Sept. 2006, avail. from www.benfieldgroup.com.

Chang, C.-P., and G. T.-J. Chen, 1995: Tropical circulations associated with the southwest monsoon onset and westerly surges over the South China Sea, *Mon. Wea. Rev.*, 123, 3254-3267.

Emanuel, K., 2005, *Divine Wind: The History and Science of Hurricanes*. Oxford University Press, New York, 285 pp.

Guy Carpenter, 2006: *Typhoon Saomai: Impact and Historical Comparison*. Nov. 2006, 32 pp.

International Insurance Fact Book 2006-07. Insurance Information Institute, 110 William Street, New York, NY 10038, 115 pp.

Jones, S. C., P. A. Harr, J. Abraham, L. F. Bosart, P. J. Bowyer, J. L. Evans, D. E. Hanley, B. N. Hanstrum, R. E. Hart, F. Lalurette, M. R. Sinclair, R. K. Smith, and C. Thorncroft, 2003: The Extratropical Transition of Tropical Cyclones: Forecast Challenges, Current Understanding, and Future Directions, *Wea. Forecast.*, 18, 1052-1092.

Kentang, L., 2000: An Analysis of the Recent Severe Storm Surge Disaster Events in China. *Natural Hazards* 21: 215-223.

Yihong, D., 2006: Typhoons Bilis and Saomai: why the impacts were so severe. *WMO Bulletin*, 55(4), 280-284. This report is available online from: http://www.wmo.int/pages/publications/bulletin/documents/Bulletin55_4.pdf

Quing, D., J. G. Thibodeau, P. B. Williams, and M. Yi, 1997: *The River Dragon Has Come!: The Three Gorges Dam and the Fate of China's Yangtze River and Its People*. Probe International and International Rivers Network. 270 pp.